European Journal of Neuroscience, Vol. 14, pp. 927–936, 2001

ATP stimulation of $P2X_7$ receptors activates three different ionic conductances on cultured mouse Schwann cells

Aurore Colomar and Thierry Amédée
Institut National de la Santé et de la Recherche Médicale U394, Neurobiologie Intégrative, Institut François Magendie, Rue Camille Saint-Saëns, 33077 Bordeaux Cedex, France

Keywords: ATP, Ca^{2+}-activated K^+ current, Cl^- conductance, $P2X_7$ receptor, Schwann cell

Abstract

Extracellular ATP, by acting on P2 purinergic receptors, is a potent mediator of cell-to-cell communication both within and between the nervous and the immune systems. We show here by patch-clamp recording, fluorescent dye uptake and immunocytochemistry that, in cultured mouse Schwann cells, ATP activates a $P2X_7$ receptor associated with three different ionic conductances. In control conditions, ATP activated an inward current (I_{ATP}) with a low potency (EC_{50}, 7.2 mM). Replacing ATP either by the ATP analogue 2′,3′-*O*-(4-benzoyl-4-benzoyl)-ATP (BzATP) or by the tetraacidic form ATP^{4-} potentiated the inward current (ATP^{4-} EC_{50}, 375 μM). ATP and BzATP currents were strongly reduced by periodate oxidized ATP (oATP), an antagonist of $P2X_7$ receptors. I_{ATP} was a mixed current composed of a nonselective cationic conductance, a cationic conductance selective for K^+ and an anionic conductance selective for Cl^-. The activation of the K^+ conductance was dependent on an influx of Ca^{2+}, and was blocked by charybdotoxin (ChTX) and tetraethylammonium (TEA), two potent antagonists of large conductance Ca^{2+}-activated K^+ channels (BK channels). The activation of the Cl^- conductance was insensitive to Ca^{2+} but required the presence of K^+. Total removal of K^+ blocked both the Ca^{2+}-activated K^+ conductance and the Cl^- conductance, unveiling the $P2X_7$ nonselective cationic conductance. The $P2X_7$ receptor was localized by immunocytochemistry using a polyclonal antibody, anti-$P2X_7$, whilst its expression and functionality were both detected by the uptake of Lucifer Yellow. This receptor could regulate the synthesis and the release of cytokines by Schwann cells during pathophysiological events.

Introduction

Within the peripheral nervous system (PNS), adenosine 5′-triphosphate (ATP) is a key molecule of cell-to-cell communication. Cellular effects of extracellular ATP are mediated via P2 receptors which are subdivided into G protein-coupled receptors (P2Y) termed metabotropic receptors and receptors that directly gate ion channels (P2X) termed ionotropic receptors (see Ralevic & Burnstock, 1998). Both subtypes are expressed by mammalian Schwann cells (see Amédée *et al*., 2001).

Among the P2X family, the $P2X_7$ receptor displays amazing pleïotropic effects. On one hand, the $P2X_7$ receptor mediates cytotoxicity in lymphocytes (Wiley *et al*., 1998), microglial cells (Ferrari *et al*., 1997a) and dendritic cells (Coutinho-Silva *et al*., 1999). On the other hand, it plays a pivotal role in different processes relevant to the inflammatory response and immunomodulation. $P2X_7$ receptors regulate the synthesis and the release of cytokines by immune cells such as macrophages and microglial cells (DiVirgilio *et al*., 1998), but also by fibroblasts (Solini *et al*., 1999). Through feedback loops, pro-inflammatory cytokines such as interferon-gamma (IFNγ) and tumour necrosis factor alpha (TNFα) up-regulate the expression of $P2X_7$ receptors in human monocytes (Humphreys & Dubyak, 1996, 1998). Last, the antigen-presenting activity of mouse dendritic cells is positively linked to the expression of $P2X_7$ receptors (Mutini *et al*., 1999).

Electrophysiological studies either in native or recombinant systems have highlighted some hallmarks of $P2X_7$ receptors. These receptors form a nonselective cationic channel. The ATP-activated current shows negligible desensitization and displays a linear current–voltage relationship with a reversal potential (E_{ATP}) close to 0 mV. For long-lasting application of ATP (a few tens of seconds), the pore undergoes dilation as revealed by an increase in the permeability to large cations (Virginio *et al*., 1999). Last, the $P2X_7$ receptor displays a very low sensitivity to extracellular ATP. Up to now, the existence of low sensitivity responses to extracellular ATP and therefore mediated by $P2X_7$ receptors has been reported in only few Schwann cells species. Vinogradova *et al*. (1994) reported that, in cultured frog Schwann cells, extracellular ATP (1–10 mM) was activating a nonspecific cationic conductance. In cultured mouse Schwann cells, external ATP (EC_{50}, 8.4 mM) activated a mixed current composed of K^+ and Cl^- conductances (Amédée & Despeyroux, 1995). Last, on rat Schwann cells, Grafe *et al*. (1999) reported the expression of a ionotropic purinergic receptor displaying some of the electrophysiological and pharmacological characteristics of the $P2X_7$ subtype.

In the present work we have looked for the expression of $P2X_7$ receptors and associated ionic conductances in cultured mouse Schwann cells. We report that mouse Schwann cells express a $P2X_7$ receptor whose activation opens a nonselective cationic channel and two associated conductances: a Ca^{2+}-dependent K^+ conductance

Correspondence: Dr Thierry Amédée, as above.
E-mail: Thierry.Amedee@bordeaux.inserm.fr

Received 5 April 2001, revised 25 June 2001, accepted 16 July 2001

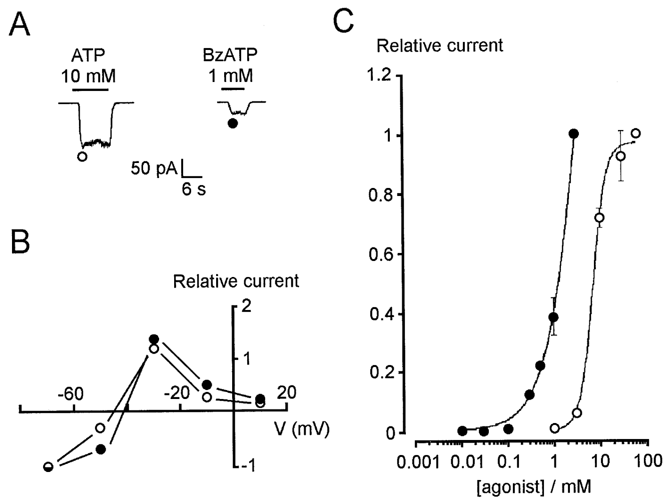

FIG. 1. ATP- and BzATP-activated currents in mouse Schwann cells. (A) Representative currents activated by ATP (10 mM) and BzATP (1 mM) were recorded on the same cell from a holding potential of –70 mV. Note that the currents were maintained during the application of both agonists. (B) Current–voltage relationships for I_{ATP} (○) and I_{BzATP} (●) on the same cell as shown in A. Note that the two curves displayed a similar voltage dependence. The reversal potential was –45 mV for I_{ATP} and –42 mV for I_{BzATP}. For the sake of clarity I_{ATP} and I_{BzATP} have been scaled to the amplitude of their respective currents recorded from –70 mV. (C) The peak current amplitude activated by each concentration of ATP (○) was normalized to that elicited by 30 mM ATP. The curve for I_{ATP} was calculated from the following equation: $I_{[ATP]}/I_{[ATP\infty\_]} = 0.97/[1 + (K/[ATP])^{n_H}]$. The number of data at each concentration were $n = 4$ (1 mM), $n = 16$ (3 mM), $n = 15$ (10 mM), $n = 7$ (30 mM) and $n = 5$ (60 mM). The best-fit curve gave EC_{50}, 7.2 mM and $n_H = 2.8$. For BzATP, the peak current amplitude (●) was normalized to that elicited by 3 mM BzATP. The curve was fitted by eye. The number of data at each concentration were $n = 15$ (0.01 mM), $n = 18$ (0.03 mM), $n = 17$ (0.1 mM), $n = 19$ (0.3 mM), $n = 13$ (0.5 mM), $n = 12$ (1 mM) and $n = 6$ (3 mM). The holding potential was –70 mV and error bars are ± SEM.

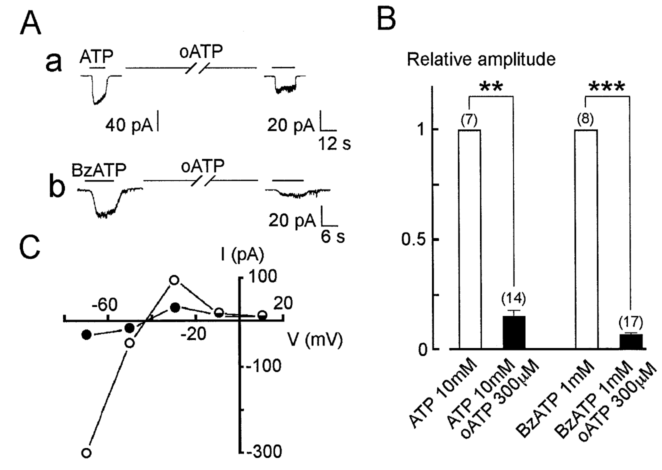

FIG. 2. Effects of oATP on ATP- and BzATP-activated currents. (A) Representative currents activated by either (a) 10 mM ATP or (b) 1 mM BzATP recorded from different cells in control conditions and following a pretreatment by oATP (300 µM) for 90 min. oATP strongly decreased I_{ATP} and I_{BzATP}. Note the different scale bar for the amplitude of I_{ATP} after the pretreatment by oATP. Holding potential –70 mV. (B) The open columns show the relative amplitude of I_{ATP} and I_{BzATP} in control conditions and are normalized to 1. The filled columns show the relative amplitude of I_{ATP} and I_{BzATP} after a pretreatment by oATP (300 µM) for 90 min. $^{**}P < 0.01$ and $^{***}P < 0.001$ using Student's paired *t*-test. (C) Current–voltage relationships obtained in two different cells for I_{ATP} in control conditions (○) and after a pretreatment by oATP (300 µM) for 90 min (●). Note that the two curves displayed similar voltage dependence and reversal potentials.

which is suppressed in Ca^{2+}-free bathing solution and blocked by internal BAPTA, and a Cl^- conductance whose functioning requires the presence of K^+.

Materials and methods

Glial cell cultures

Schwann cells were cultured from excised dorsal root ganglia from OF1 mouse embryos (E19) as previously described (Amédée *et al*., 1991; Beaudu-Lange *et al*., 1998). Mice were killed by decapitation. Briefly, dorsal root ganglia were isolated from embryos and plated onto 35-mm Petri dishes (Nunc, Roskilde, Denmark) coated with rat tail collagen (Collagen R, Serva, Heidelberg, Germany). Cells were cultured in α-modified Eagle's medium (α-MEM, Gibco, Cergy-Pontoise, France) containing nerve growth factor (20 ng/mL; Euromedex, Souffelweyersheim, France). The medium was changed twice a week and cells were used between 2 and 6 weeks of culture for electrophysiology, membrane permeabilization and immunocytochemistry experiments.

Microglial cells were used as a positive control for the expression of $P2X_7$ receptors (Ferrari *et al*., 1996; Haas *et al*., 1996). They were cultured from newborn mice (1–3 days) as described in detail by Pousset *et al*. (2000). Mice were killed by decapitation. Brains were dissected and placed in Dulbecco's modified Eagle's medium (DMEM, Gibco). The meningeal tissue was stripped off. Brains were mechanically dissociated and the resulting cell suspension was passed through a sterile nylon mesh (70 µm, Falcon, Plymouth, England). Cells were plated at a density of 5×10^4 cells per dish into DMEM containing 20% heat-inactivated fetal calf serum (Boehringer Mannheim, Indianapolis, USA; < 10 pg/mL endotoxins). Under these conditions, neurons do not survive the mechanical dissociation, and the low plating density prevents oligodendrocyte proliferation. After four weeks in culture, enriched microglial cells were obtained by intense washing of mixed glial cell cultures which have been deprived of serum for 48 h. Enriched microglial cell culture consisted of 95% microglia and 5% astrocytes as determined by immunofluorescence staining and cell count.

Electrophysiology

Currents were recorded from Schwann cells cultured for 2–6 weeks by using the whole-cell configuration of the patch-clamp technique at room temperature (20–24 °C). Patch pipettes were pulled from borosilicate glass capillaries (GF 150 TF-10, Clark Electromedical Instruments, Pangbourne, UK) and filled with an internal solution containing (in mM): KCl, 120; $CaCl_2$, 1; $MgCl_2$, 2; HEPES, 10; ethyleneglycol-bis (β-aminoethylether)-N,N′-tetraacetic acid (EGTA), 10; glucose, 11; NaOH, 5; and KOH, 33 (pH 7.4). In some experiments, EGTA was replaced in the internal solution by 1,2-bis (2-aminophenoxy) ethane-N,N,N',N′-tetraacetic acid (BAPTA). In control conditions, patch pipettes had resistances of 5–10 MΩ. Voltage-clamp protocols were applied from a holding potential of –70 mV by using a L/M-EPC-7 patch-clamp amplifier (List-Electronic, Darmstadt, Germany). Signals were stored on a digital audio tape recorder (DTR-1200, Biologic, Grenoble, France) at a sampling frequency of 48 kHz and displayed on a chart recorder. Whole-cell currents were sampled at 125 kHz by a TL–1 interface (Axon Instruments, Foster City, USA).

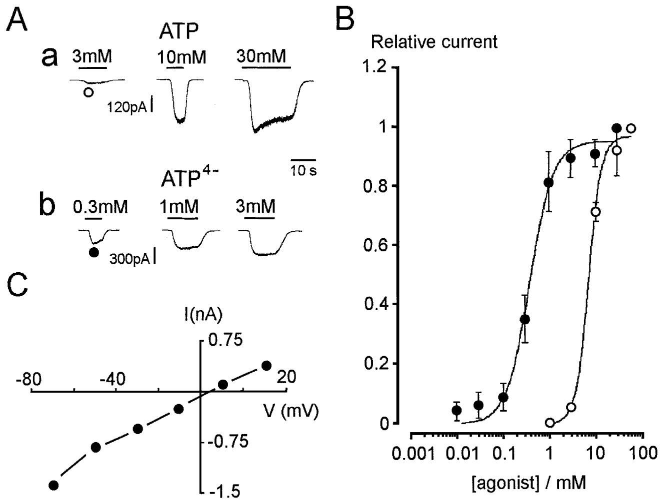

FIG. 3. ATP- and ATP^{4-}-activated currents. (A) Family of typical current traces activated by increasing concentrations of (a) ATP recorded on the same cell and (b) same protocol with ATP^{4-}. Holding potential –70 mV. Note that replacing ATP by ATP^{4-} produced a pronounced enhancement of the inward current. (B) The peak current amplitude activated by each concentration of ATP^{4-} (●) was normalized to that elicited by 30 mM ATP^{4-}. The curve was calculated from the following equation: $I_{[ATP4-]}/I_{[ATP4-\infty]} = 0.95/[1 + (K/[ATP^{4-}])^{nH}]$. The number of data at each concentration were $n = 5$ (0.01 mM), $n = 5$ (0.03 mM), $n = 5$ (0.1 mM), $n = 13$ (0.3 mM), $n = 7$ (1 mM), $n = 8$ (3 mM), $n = 8$ (10 mM) and $n = 8$ (30 mM). The best-fit curve gave EC_{50}, 375 μM and $n_H = 2.2$. The holding potential was –70 mV and error bars are ± SEM. For an easiest comparison, the concentration–response curve for I_{ATP} (○), same as shown in Fig. 1C, was plotted on the same graph. (C) Current–voltage relationship for I_{ATP4-}. The reversal potential was 5 mV. Note the suppression of the inward rectification.

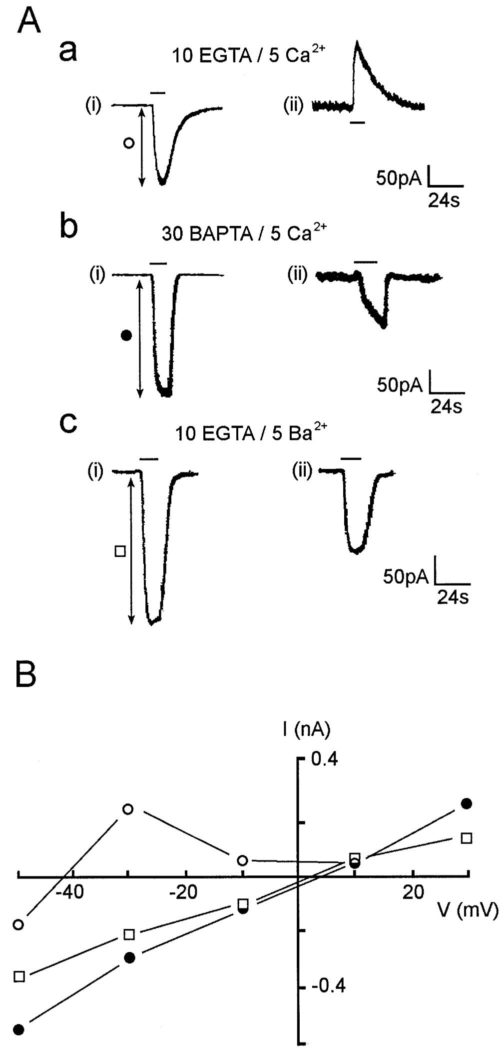

FIG. 4. Dependence of the K^+ conductance on extracellular Ca^{2+}. (A) ATP 10 mM was applied at (i) –50 mV and (ii) –30 mV using either EGTA or BAPTA in the pipette solution and Ca^{2+} or Ba^{2+} in the bathing solution. (a) With 10 mM EGTA/5 mM Ca^{2+}, I_{ATP} was inward at –50 mV and outward at –30 mV. (b) Replacing 10 mM EGTA by 30 mM BAPTA in the pipette solution produced the reversal of I_{ATP} at –30 mV. (c) Replacing 5 mM Ca^{2+} by 5 mM Ba^{2+} in the bathing solution (in the presence of 10 mM EGTA in the pipette solution) also produced the reversal of I_{ATP} at –30 mV. (B) Typical current–voltage relationships for I_{ATP} in control conditions (○), with 30 mM BAPTA (●) and with 5 mM Ba^{2+} (□). Note the suppression of the marked inward rectification when the K^+ conductance was blocked.

Junction potentials and series resistance errors

When most of the Cl^- (140 mM) was replaced by large organic anions to leave 17 mM Cl^-, significant changes in junction potential were likely to arise and alter the value of the reversal potential. Therefore, the junction potential was estimated according to the following procedure: the pipette potential was set at 0 mV when the pipette was placed in the bathing solution where Cl^- was replaced by another large organic anion. An agar bridge (5% w/v in 150 mM KCl) was used as a bath electrode. The bathing solution was then replaced by the pipette solution (to mimic the establishment of the whole-cell configuration) and the change in potential measured ($\Delta V = 1.1 \pm 1.07$ mV, $n = 10$). Therefore no corrections of the reversal potential were made.

Values for the ATP reversal potentials were obtained from current amplitudes within the range –50 to –600 pA. In the whole-cell recording mode, a mean value of 8 MΩ (7.9 ± 4.9 MΩ, $n = 4$) was measured for the series resistance. Therefore errors in potential due to series resistance were within the range 0.4–5 mV and no correction was applied.

External solutions and purine application

In control conditions, the bathing solution was (in mM): NaCl, 140; $CaCl_2$, 5; $MgCl_2$, 2; HEPES, 10; glucose, 11; and NaOH, 4 (pH 7.4). Nominal Ca^{2+}- and Mg^{2+}-free solution was obtained by omitting these cations from the bathing solution. Acute application of ATP and related analogues to Schwann cells was achieved by a perfusion system based on electromagnetic valves controlling gravity flow. A flow manifold which established a common outlet for the different flow lines was mounted on a hydraulic micromanipulator. To minimize mechanical perturbation to the cell which sometimes arose when changing flow lines, the common outlet was placed at ≈ 500 μm away from cells. Stock solution for ATP and related analogues were prepared and stored at –20 °C. On the day of experiment, fresh solutions were made from stock solutions and the pH was readjusted to 7.4. Because of a limited solubility in standard external solution, 3 mM was the highest concentration of BzATP that we achieved. The following drugs were used: ATP (A-2383), BzATP (B-6396), oATP (A-6779), Lucifer Yellow (L-3510) and tetraethylammonium (TEA) (T-2265), all from Sigma, and charybdotoxin (L8213) from Latoxan (Valence, France).

Studies of the permeabilization of the plasma membrane

Changes of the plasma membrane permeability were measured with the extracellular fluorescent dye Lucifer Yellow (Sigma, Saint Quentin Fallavier, France). Cell cultures were incubated for 15 min at 37 °C with Lucifer Yellow (1 mg/mL) either in standard external solution containing ATP or in nominal Ca^{2+}- and Mg^{2+}-free solution for stimulation by ATP^{4-}. In some experiments, cell cultures were preincubated with oATP (300 μM) for 90 min. Then cell cultures were washed several times to remove all the extracellular dye, and were observed using an inverted microscope (Nikon Diaphot, Champigny sur Marne, France) equipped with a ×60 objective. Fluorescence was monitored using an excitation filter (wavelength 400–440 nm) and a barrier filter (wavelength 480 nm).

Immunocytochemistry

$P2X_7$ receptors were stained with a polyclonal antibody raised in rabbit against highly purified peptide corresponding to residues 576–595 of rat $P2X_7$ (Alomone Laboratories, Jerusalem, Israel). The cell cultures were rinsed with phosphate buffered saline (PBS), fixed with paraformaldehyde (4% in PBS) for 30 min, permeabilized with Triton (0.1%) for 15 min, then rinsed with PBS. Nonspecific binding sites were saturated with PBS supplemented with 0.25% bovine serum albumin (BSA; Sigma) and 0.2% gelatin (Merck, Darmstadt, Germany) for 45 min. The primary antibody, i.e. anti-$P2X_7$, was applied overnight at 4 °C at a dilution of 1 : 200. The cell cultures were then rinsed and incubated for 90 min with the second antibody [goat antibody against rabbit IgG, biotinylated, Biosys, Compiègne, France] at a dilution of 1 : 500. Cell cultures were incubated with

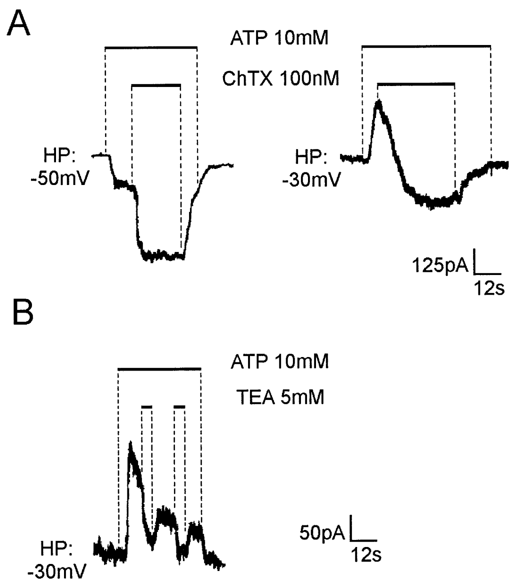

FIG. 5. Effects of two Ca^{2+}-activated K^+ channels blockers, ChTX and TEA, on I_{ATP}. (A) ATP 10 mM was applied at –50 mV and –30 mV. The simultaneous application of ChTX (100 nM) by blocking the outward Ca^{2+}-activated K^+ current of I_{ATP} enhanced the inward current at –50 mV whereas it reversed from outward to inward at –30 mV (n = 5). (B) In another cell, the repetitive application of TEA (5 mM) on the ATP-activated current partially and reversibly decreased the outward component of I_{ATP} at –30 mV (n = 4).

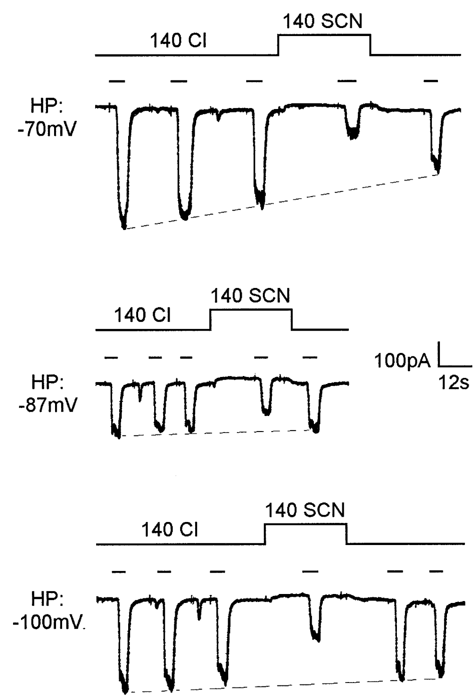

FIG. 6. Lack of interaction between the direction of K^+ fluxes and the Cl^- conductance. The repetitive application of ATP (10 mM) was performed prior to the external replacement of Cl^- by SCN^- in order to estimate the percentage of rundown of I_{ATP} (illustrated by the dotted line). All experiments were carried out in the absence of extracellular Ca^{2+} (substituted by Ba^{2+}) to eliminate the Ca^{2+}-activated K^+ current. The same cell was recorded successively from –70, –87 and –100 mV. Note that the amplitude of I_{ATP} was reduced by the external replacement of Cl^- by SCN^- (see text for a detailed explanation) whatever the direction of K^+ fluxes, i.e. outwardly directed at –70 mV, null at –87 mV and inwardly directed at –100 mV.

FIG. 7. Morphological alterations and membrane permeabilization induced by ATP. (A) Phase contrast and fluorescence illumination micrographs of cultured mouse Schwann cells in control conditions. Schwann cells had oval shaped bodies (arrowheads) with thin processes (a) and no Lucifer Yellow uptake was detectable (b). (B) ATP 10 mM induced the rounding of Schwann cell bodies (white arrowheads) and blebbing of processes (black arrowheads) (a) together with an intense Lucifer Yellow uptake (b). (C) A pretreatment with oATP (300 μM, 90 min) totally blocked morphological changes (a) and membrane permeabilization (b) induced by ATP (10 mM). Scale bar, 100 μm.

FIG. 8. Immunocytochemical staining of the $P2X_7$ receptor with a fluorescein-conjugated secondary antibody. In all figures, cultures have been counterstained with Evans Blue which gives a red signal. (A) In organotypic cultures, both isolated Schwann cell and those associated with neurites were positively stained (yellow fluorescence) by the $P2X_7$ antibody. In contrast, neurites were $P2X_7$-negative. (B) As a negative control, the $P2X_7$ antibody was replaced by PBS. In these conditions, only Evans Blue counterstaining (red signal) was detectable in Schwann cells and neurites. (C) In order to assess the specificity of the immunostaining, the $P2X_7$ antibody was preadsorbed with the control antigen. No nonspecific immunostaining was detectable. (D) As a positive control, the immunostaining was performed on mouse microglial cells which express $P2X_7$ receptors. Note that all microglial cells were $P2X_7$-positive. Scale bar, 25 μm.

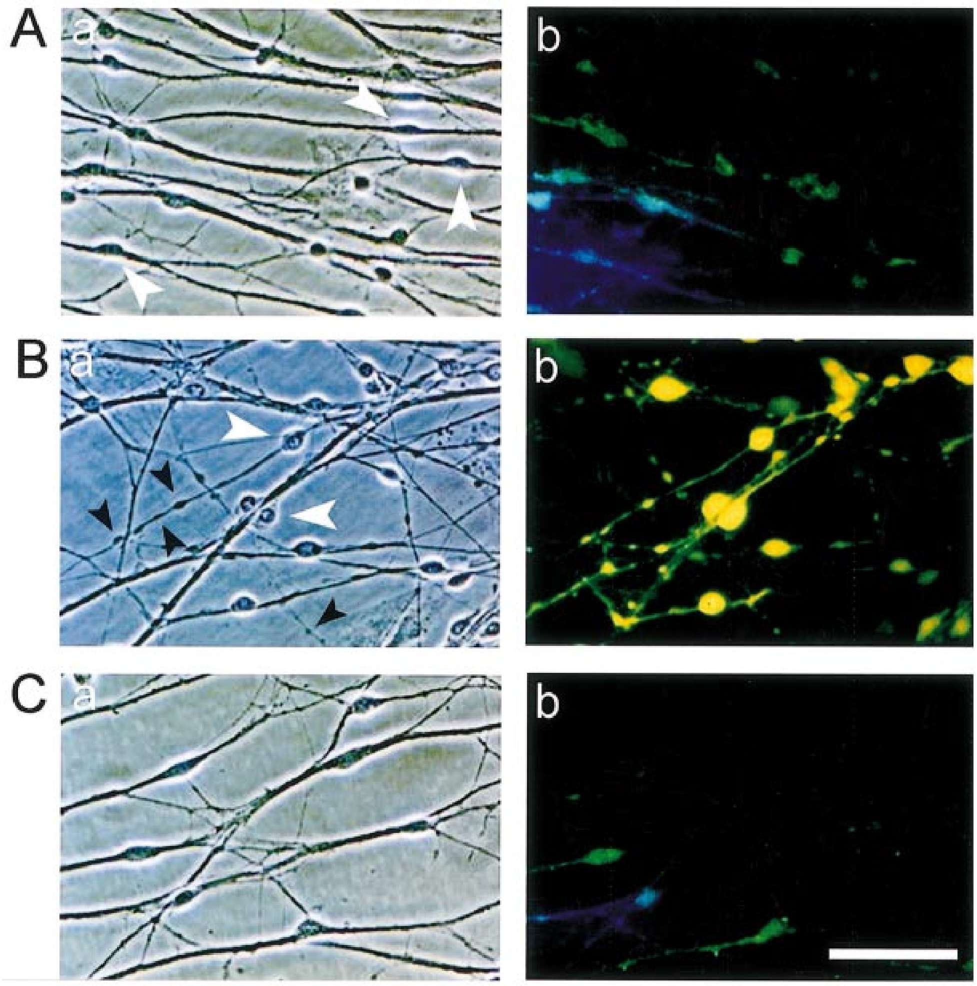

FIG. 7.

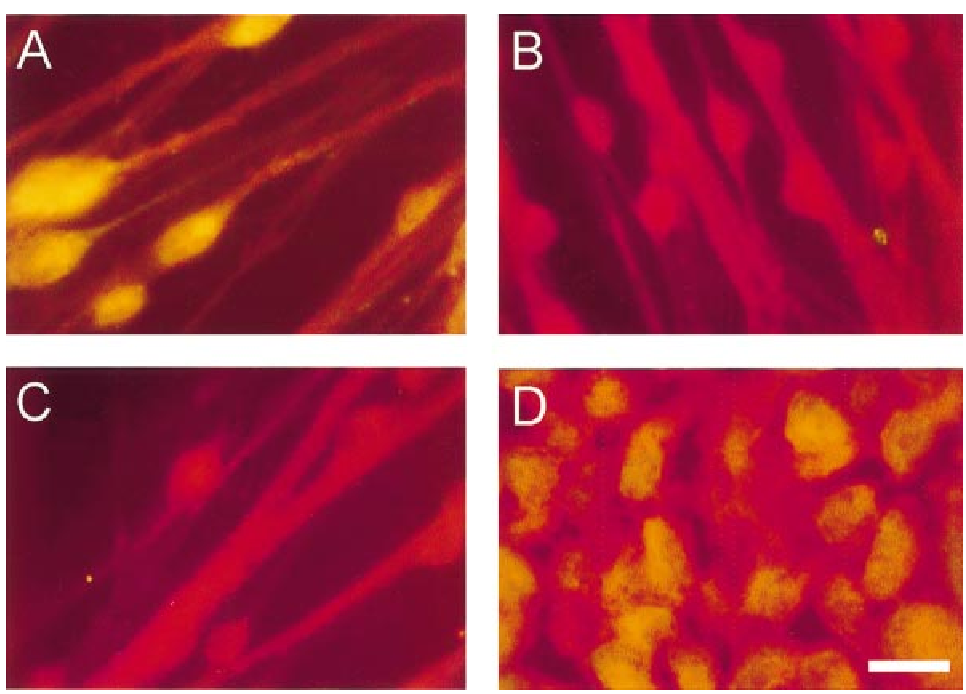

FIG. 8.

FITC streptavidin at a dilution of 1 : 200, counterstained with Evans blue (40% w/v), then rinsed and observed under fluorescence microscopy (Leica Med, emission wavelength 450–490 nm; barrier filter wavelength 520 nm) equipped with a ×100 objective. Vectashield (Vector, Burlingame, USA) was added to stop photobleaching.

Data analysis

Concentration-dependent data were fitted using the equation $I_{[ATP]}/I_{[ATP\infty\_]} = A/[1 + (K/[ATP])^{n_H}]$ in which K is the EC_{50} and n_H the Hill coefficient. Results in the text are expressed as mean ± SEM and significance was tested by means of Student's paired *t*-test and assessed at $P < 0.05$.

Results

Evidence for the activation of a $P2X_7$ receptor by ATP and ATP analogues on cultured mouse Schwann cells

In a control bathing solution, from a holding potential of –70 mV, external application of ATP (1–30 mM) activated in >95% of Schwann cells an inward current (I_{ATP}) which was almost maintained during the application of ATP (Fig. 1A). With 10 mM ATP, the peak current amplitude of I_{ATP} ranged from –110 to –640 pA and the mean value was –271 ± 90 pA (n = 16). In most cells, repetitive application of ATP did not produce noticeable desensitization (rundown) of I_{ATP}. Fig. 1B shows a representative current–voltage relationship. The mean reversal potential (E_{ATP}) of the current was –45.9 ± 1.5 mV (n = 16). The peak amplitude of I_{ATP} increased in a concentration-dependent manner and the experimental data were best fitted by a curve with an EC_{50} of 7.2 mM (Fig. 1C). We then studied the effect of the ATP analogue 2′,3′-*O*-(4-benzoyl-4-benzoyl) (BzATP) which is described as a more potent agonist for $P2X_7$ receptors than ATP, both in recombinant and in native systems (Ralevic & Burnstock, 1998). As shown in Fig. 1A, the mean amplitude of I_{BzATP} (1 mM) represented ≈ 36% of the mean amplitude of I_{ATP} (10 mM) whilst the mean amplitude of I_{ATP} (1 mM) represented only 1.5% of the mean amplitude of I_{ATP} (10 mM). I_{BzATP} displayed the same voltage dependence as I_{ATP} (Fig. 1B). The mean reversal potential E_{BzATP} was not significantly different from E_{ATP} (E_{BzATP} = –37.5 ± 5.3 mV, n = 8, $P > 0.05$). The concentration–response relationship for the peak amplitude of I_{BzATP} (Fig. 1C) was shifted towards lower concentrations with respect to that obtained for I_{ATP}. Unfortunately, because of a limited solubility of BzATP in the control bathing solution, we could not obtain the maximal response to BzATP which precluded any precise calculation of the EC_{50}. However, from the concentration–response relationship, the EC_{50} could be estimated to ≈ 1 mM.

We tested then the effects of periodate oxidized ATP (oATP), described as an irreversible antagonist at the $P2X_7$ receptor, on I_{ATP} (Fig. 2A, a) and on I_{BzATP} (Fig. 2A, b). Both currents were strongly reduced by a preincubation for 90 min with oATP (300 μM). I_{ATP} (10 mM) was reduced by 86 ± 3% (n = 14) and I_{BzATP} (1 mM) was reduced by 93 ± 5% (n = 17) (Fig. 2B). Figure 2C shows the current–voltage relationships for I_{ATP} in control conditions and after the preincubation with oATP. Both curves had the same shape without a significant change of E_{ATP} (control –45.9 ± 1.5, n = 16; in the presence of oATP –43.8 ± 9.6 mV, n = 5, $P > 0.05$) suggesting that ATP and oATP were acting on the same purinergic receptor.

Last, we studied the effect of ATP^{4-} because this tetraacidic form of ATP is described as the physiological and specific agonist of $P2X_7$ receptors. In a control bathing solution, ATP is almost entirely complexed to divalent cations (Ca^{2+} and Mg^{2+}). To increase the relative concentration of ATP^{4-} over ATP, we replaced the control bathing solution by a Ca^{2+}- and Mg^{2+}-free bathing solution. Figure 3A shows that indeed ATP^{4-} was more potent than ATP in activating an inward current (I_{ATP4-}) from a holding potential of –70 mV. The mean amplitude of I_{ATP4-} (1 mM) represented ≈ 80% of the mean amplitude of I_{ATP} (10 mM). As for the agonist BzATP, the concentration–response curve for I_{ATP4-} was shifted towards lower concentrations. The best fit gave an EC_{50} of 375 μM (Fig. 3B). Using a Ca^{2+}- and Mg^{2+}-free bathing solution produced striking changes in the current–voltage relationship of I_{ATP4-} with respect to I_{ATP} and I_{BzATP}. The mean E_{ATP4-} was significantly shifted towards positive values (+6.2 ± 2.7 mV, n = 8, $P < 0.001$) and the current–voltage relationship became almost linear (Fig. 3C). Altering the Na^+ gradient by replacing half of the extracellular Na^+ by Tris did not significantly changed E_{ATP4-} (+3.2 ± 4.5 mV, n = 5, $P > 0.05$), suggesting similar permeabilities for Na^+ and Tris through the $P2X_7$ pore.

One the one hand, the potentiation of the ATP-activated current by BzATP and ATP^{4-}, its blockade by oATP and the electrophysiological properties of I_{ATP4-} (linearity of the current–voltage relationship, mean value of E_{ATP4-}, permeability to cations) are all consistent with the activation of a $P2X_7$ receptor. But on the other hand, in control bathing solution the mean reversal potential for either I_{ATP} or I_{BzATP} correspond neither to the sole activation of a $P2X_7$ nonselective cationic current (which should predictably reversed close to 0 mV), nor to the theoretical values for equilibrium potential of any of the ions present (E_{K+} = –87 mV, E_{Cl-} = –6 mV, E_{Na+} = +84 mV, E_{Ca2+} = +135 mV). This is consistent with the activation, downstream of the $P2X_7$ receptor, of a cationic conductance permeable to K^+ ions and a separate anionic conductance permeable to Cl^- ions (Amédée & Despeyroux, 1995).

Ca^{2+}-dependence of the cationic conductance selective for K^+ ions

With 30 mM BAPTA in the pipette solution I_{ATP} reversed from outward (Fig. 4A, aii) to inward (Fig. 4A, bii) at –30 mV. E_{ATP} was significantly shifted to more positive values (control E_{ATP} = –45.9 ± 1.5 mV, n = 19; BAPTA E_{ATP} = +14.4 ± 4.6 mV, n = 7, $P < 0.001$) and the inward rectification was suppressed (Fig. 4B). Because under these ionic conditions the only ion able to carry a net outward current at –30 mV was K^+, we interpreted these results as good evidence that BAPTA blocked a Ca^{2+}-activated K^+ current, unveiling therefore the involvement of Ca^{2+}-activated K^+ channels in I_{ATP}. However, these results did not distinguish between the two main possible sources of Ca^{2+} that could activate the K^+ conductance, i.e. the influx of extracellular Ca^{2+} and/or the release of Ca^{2+} from intracellular stores. To investigate this issue, we replaced extracellular Ca^{2+} by Ba^{2+} and found that this replacement produced the same effects as intracellular buffering of Ca^{2+} by 30 mM BAPTA, that is an inwardly directed I_{ATP} at –30 mV (Fig. 4A, cii), a shift of E_{ATP} (E_{ATP} = +5.1 ± 1.9 mV, n = 7) and the suppression of the inward rectification (Fig. 4B).

From these results we concluded that the activation of the Ca^{2+}-activated K^+ conductance required the presence of external Ca^{2+} which suggested a major role for a Ca^{2+} influx. We then tested the effects on I_{ATP} of charybdotoxin (ChTX) and TEA, two well known blockers of the large conductance Ca^{2+}-activated K^+ channel (BK channel). When applied from a holding potential of –50 mV, ChTX (100 nM) increased the amplitude of I_{ATP} whereas, when applied at –30 mV, it reversed I_{ATP} from outward to inward (Fig. 5A). Similar effects, although less pronounced, were obtained with external application of 5 mM TEA (Fig. 5B). These results were consistent with the blockade (or the strong reduction) of a Ca^{2+}-activated K^+ current of the BK type (outwardly directed at both –50 and –30 mV) leading therefore to a larger inward current at –50 mV and to its reversal at –30 mV.

Lack of Ca^{2+}-dependence of the Cl^- conductance

In Ca^{2+}-free bathing solution, I_{ATP} may result from an inward movement of cations through the $P2X_7$ nonselective cationic pore itself, or alternatively from an outward movement of Cl^- through the anionic conductance activated downstream of the $P2X_7$ receptor, or even from a mixture of both. To distinguish between these different possibilities, we checked whether the Cl^- conductance was still activated by ATP in Ca^{2+}-free bathing solution by altering the anionic gradient. When extracellular Ca^{2+} was substituted by Ba^{2+}, the replacement of most of external Cl^- by thiocyanate (SCN^-), which is more permeant through the ATP-activated Cl^- conductance (permeability ratio $P_{SCN}/P_{Cl} = 9.0$; Amédée & Despeyroux, 1995), shifted E_{ATP} significantly towards more negative values (E_{ATP} = –40.6 ± 2.1 mV, $n = 5$, $P < 0.001$). This negative shift of E_{ATP} suggested that the Cl^- conductance could still be activated by ATP in the absence of extracellular Ca^{2+}. Intracellular buffering of Ca^{2+} ions by 30 mM BAPTA gave similar results (not shown). We concluded therefore that, in contrast to the Ca^{2+}-activated K^+ conductance, the gating mechanism of the Cl^- conductance did not rely on an influx of Ca^{2+} ions.

Evidence for an interaction between K^+ ions and the Cl^- conductance

As previously reported (Amédée & Despeyroux, 1995) and confirmed by the present work, the suppression of the Ca^{2+}-activated K^+ conductance by K^+-free bathing and pipette solutions shifted E_{ATP} by >40 mV (E_{ATP} = –0.7 ± 1.1 mV, $n = 6$). But surprisingly under these ionic conditions, the external replacement of Cl^- by SCN^- did not modified E_{ATP} (E_{ATP} = +1 ± 1.5, $n = 6$, $P > 0.05$) as expected from a functional Cl^- conductance. This indicates therefore that the Cl^- conductance requires K^+ ions to be functional and sets experimental conditions where I_{ATP} seems to be only due to the $P2X_7$ nonselective cationic conductance.

We then studied whether the permissive effect of K^+ ions on the Cl^- conductance involved K^+ fluxes across the plasma membrane by setting the direction of the net movement of K^+ ions (i.e. entering or leaving the cell) using three different holding potentials (–100, –87 and –70 mV). As E_{K+} = –87 mV, the net movement of K^+ ions is inwardly directed at –100 mV, outwardly directed at –70 mV and negligible at –87 mV. The rationale of the experiment is based on the decrease of the relative amplitude of the Cl^-component of I_{ATP}, due to the shift of the reversal potential towards more negative values when Cl^- is replaced by SCN^-. If, for the three different holding potentials, the amplitude of I_{ATP} is reduced with SCN^- with respect to its amplitude with Cl^-, then this is good evidence that the functioning of the anionic conductance does not depend on a preferential direction of K^+ fluxes. However, if for example the Cl^- conductance relies on an efflux of K^+ to be functional, the amplitude of I_{ATP} with SCN^- should be reduced at –70 mV (when the Cl^- conductance is functional) but unchanged at –87 and –100 mV (when the Cl^- conductance is not functional) with respect to its amplitude with Cl^-. As shown in Fig. 6, the amplitude of I_{ATP} was reduced when Cl^- was replaced by SCN^- whatever the value of the holding potential, indicating therefore that the interaction between K^+ and the Cl^- conductance was not linked to the driving force for K^+.

Morphological changes and plasma membrane permeabilization induced by $P2X_7$ receptor stimulation

The functional expression of the $P2X_7$ receptor was studied by monitoring both the morphological changes and the membrane permeabilization to Lucifer Yellow induced by extracellular ATP and ATP^{4-}. To be consistent with the electrophysiological data, we used concentrations of ATP and ATP^{4-} close to their respective EC_{50} values. In control conditions (Fig. 7A, a), mouse Schwann cells had small and spindle-shaped oval bodies with narrow tapered processes at each end when not associated with neurites (we named this phenotype 'isolated Schwann cells'). Schwann cells which were associated physically with neurites also had oval bodies. The incubation of organotypic cultures with 10 mM ATP for 15 min produced striking morphological changes in mouse Schwann cells. The oval bodies of Schwann cells became round-shaped for both phenotypes and the fine processes were blebbing (Fig. 7B, a). These morphological changes were blocked by a pretreatment with 300 μM oATP (Fig. 7C, a). In immune cells, such morphological alterations have been attributed to a dramatic membrane permeabilization due to the opening and the progressive dilation of the $P2X_7$ pore. The molecular cut-off of the $P2X_7$ receptor is ≈900 Da and therefore the induction of the uptake of Lucifer Yellow (MW 550) by exposure to extracellular ATP (or ATP^{4-}) is a convenient way to detect the presence of functional $P2X_7$ receptors. In the absence of extracellular ATP (Fig. 7A, b), no uptake of Lucifer Yellow was detectable either in Schwann cells or in neurites. In contrast, a treatment with 10 mM ATP (Fig. 7B, b) for 15 min induced the uptake of Lucifer Yellow throughout Schwann cell bodies. The membrane permeabilization induced by ATP was entirely blocked by a pretreatment with 300 μM oATP for 90 min (Fig. 7C, b). ATP^{4-} (1 mM), agonist of $P2X_7$ receptors, induced the same morphological changes and dye uptake, both blocked by oATP.

Immunocytochemical staining of $P2X_7$ receptors in mouse Schwann cells

Last we studied the cellular localization of the $P2X_7$ receptor in mouse Schwann cells by using a polyclonal antibody raised against a specific epitope of $P2X_7$ receptors. Positive immunoreactivity to the $P2X_7$ receptor antibody is revealed by a yellow staining, whereas red staining is only due to the counterstaining of cells with Evans Blue. Figure 8A showed clear immunoreactivity to the $P2X_7$ receptor antibody both in isolated Schwann cells or in Schwann cells associated with neurites. The immunoreactivity was diffuse throughout Schwann cell bodies suggesting that $P2X_7$ receptors were uniformly distributed on the plasma membrane. For negative controls, the primary antibody was omitted (Fig. 8B). The specificity of the immunostaining was tested by preadsorbtion of the $P2X_7$ receptor antibody with an excess of the control antigen peptide. In these conditions, no immunoreactivity to the $P2X_7$ receptor antibody was detectable (Fig. 8C). As microglial cells are well known to express $P2X_7$ receptors (Ferrari *et al*., 1996; Haas *et al*., 1996), we used these cells as positive control. Figure 8D shows immunoreactivity of microglial cells to the $P2X_7$ receptor antibody.

Discussion

The results presented in this study confirm and extend our previous observations (Amédée & Despeyroux, 1995), showing that external ATP activates K^+ and Cl^- conductances through the stimulation of a low sensitivity P2 purinergic receptor in cultured mouse Schwann cells. In the present study, we identified unequivocally this receptor as a $P2X_7$ receptor, whose activation switched on a Ca^{2+}-activated K^+ conductance and a Cl^- conductance linked to K^+ ions, in addition to the nonselective $P2X_7$ cationic pore.

Hallmarks of the activation of a $P2X_7$ receptor in mouse Schwann cells

First, the sensitivity to ATP (EC_{50}, 7.2 mM) is very low, but the removal of extracellular Ca^{2+} and Mg^{2+} potentiates by $\approx 20\times$ the inward current (EC_{50}, 375 μM). It is mainly attributed to the fact that ATP^{4-}, which is described as the physiological and specific agonist of the $P2X_7$ receptor, represents only 1–10% of the total ATP concentration in a physiological solution (Cohn, 1990; Ralevic & Burnstock, 1998). As a consequence, membrane responses to ATP are potentiated in a Ca^{2+}- and Mg^{2+}-free solution where the ratio ATP^{4-} : ATP increases.

Second, BzATP, which is described as the most potent agonist at endogenous $P2X_7$ receptors, potentiates the inward current. In rat Schwann cells, Grafe *et al*. (1999) reported that from a holding potential of –80 mV, ATP (1 mM) induced a current of –2.46 ± 0.5 pA/pF whilst BzATP (150 mM) induced a current of –12.69 ± 4.2 pA/pF. This yielded a relative ratio $I_{BzATP} : I_{ATP}$ of 5.16. In the present work, we calculated a relative ratio $I_{BzATP} : I_{ATP}$ of 5.02 (holding potential –70 mV). In this respect, the $P2X_7$ receptor expressed by mouse Schwann cells seemed quite similar to the $P2X_7$ receptor expressed by rat Schwann cells.

Third, oATP reduces I_{ATP} and I_{BzATP}. As oATP is a potent $P2X_7$ receptor antagonist, the lack of significant change of E_{ATP} when I_{ATP} is partially antagonized by oATP strengthens the idea that oATP binds to a sole and same receptor as ATP, that is, the $P2X_7$ receptor.

Fourth, when recorded in isolation from Ca^{2+}-activated K^+ conductance and Cl^- conductance, I_{ATP} behaves as a $P2X_7$ nonselective cationic current. As a general feature, $P2X_7$ receptors are not only permeable to monovalent (Na^+, K^+) cations but also to Ca^{2+}. In mouse Schwann cells, the Ca^{2+}-activated K^+ conductance needs external Ca^{2+} to be recruited by ATP. Under voltage-clamp protocol, the most likely and sole entry pathway for Ca^{2+} is the receptor itself, which is consistent with a significant Ca^{2+} permeability of the mouse $P2X_7$ receptor. This is in good agreement with Grafe *et al*. (1999) who reported that the rise of intracellular Ca^{2+} induced by BzATP in rat Schwann cells was entirely due to an influx of extracellular Ca^{2+} through the $P2X_7$ receptor.

Last, prolonged application of extracellular ATP or ATP^{4-} triggers plasma membrane permeabilization, rounding and blebbing of Schwann cells. Using fluorescent dye uptake and measurements of reversal potentials with extracellular cations of different sizes, Virginio *et al*. (1999) reported that activation of homomeric rat $P2X_7$ receptors led to the dilation of the cationic pore from an initial diameter of ≈ 0.8 nm to a final size of 3–5 nm within sustained stimulation. Although in the present work we have not measured these parameters, the uptake of Lucifer Yellow and the morphological changes induced by extracellular ATP or ATP^{4-} agree with the expression by mouse Schwann cells of functional $P2X_7$ receptors which form large pores during sustained activation.

In conclusion, all these results clearly show the expression of $P2X_7$ receptors by mouse Schwann cells. One may consider the possibility that functional heteromeric P2X receptors, whose pharmacological and electrophysiological properties are a blend of their respective homomeric subunits properties, could account for I_{ATP} in mouse Schwann cells. We feel that this is very unlikely as properties of known functional heteromeric P2X receptors ($P2X_{1/5}$, Torres *et al*., 1998; $P2X_{2/3}$, Lewis *et al*., 1995; $P2X_{2/6}$, King *et al*., 2000 and $P2X_{4/6}$, Lê *et al*., 1998) do not fit with the present results and moreover the expression by Schwann cells of other P2X subunits than $P2X_7$ has not been reported.

Downstream $P2X_7$ receptor-activated conductances

Low concentrations of ATP do not activate any noticeable currents in mouse Schwann cells. This is good evidence that Ca^{2+}-activated K^+ conductance and Cl^- conductance are gated downstream of the activation of the $P2X_7$ receptor. Up to now, the presence of Ca^{2+}-activated K^+ currents in mammalian Schwann cells have only been reported for cultured rat Schwann cells (Bevan *et al*., 1984). These findings have been confirmed *in situ* by immunocytochemical detection of BK channels in rat Schwann cells (Mi *et al*., 1999). In mouse Schwann cells, the pharmacology of the Ca^{2+}-activated K^+ conductance (blockade by ChTX and TEA) is consistent with the expression of Ca^{2+}-activated K^+ channels of the BK type. Because Ca^{2+}-activated K^+ currents required high concentration of intracellular BAPTA to be blocked, this may indicate that channels are located in the immediate vicinity of $P2X_7$ receptors forming microdomains where $[Ca^{2+}]$ builds up within tens of microseconds. However, it is known that Ca^{2+}-activated K^+ channels show an intrinsic voltage-dependence increasing with depolarization. Therefore in conditions where ATP may depolarize Schwann cells (Amédée & Despeyroux, 1995) the efflux of K^+ is likely to be further enhanced. To our knowledge, the existence of Ca^{2+}-activated K^+ channels whose function is coupled to $P2X_7$ receptors have not been reported in glial or immune cells. These channels form therefore a new effector for $P2X_7$ signalling in Schwann cells and represent a novel pathway for a $P2X_7$-mediated K^+ efflux.

Although the intracellular pathways linking the $P2X_7$ receptor to the Cl^- conductance were not fully characterized, it seems clear that the anion conductance does not correspond to the high conductance Cl^- channel previously described in rat Schwann cells, whose activation is only voltage-dependent (Gray *et al*., 1984; Quasthoff *et al*., 1992). However, some Cl^- pathways responding to external ATP share common characteristics with the ATP-activated Cl^- conductance described in the present study. This is the case for cystic fibrosis transmembrane regulator (CFTR)-like Cl^- currents expressed in rat submandibular gland acinar cells which are also activated downstream of the $P2X_7$ receptor activation (Zeng *et al*., 1997). Moreover, relative permeability sequences of known CFTR Cl^- channels (McCarty, 2000) are similar to the sequence in mouse Schwann cells that we reported earlier (Amédée & Despeyroux, 1995). Volume-regulated Cl^- channels can also be activated by external ATP (Pérez-Samartin *et al*., 2000) and some of them display a K^+ dependence (Steinert & Grissmer, 1997) but their kinetics are considerably slower than the ATP-activated Cl^- conductance mouse Schwann cells. Our results do not reveal the nature of the Cl^- pathway and further experiments are needed to clarify this point.

Physiological relevance of the $P2X_7$ receptor in mouse Schwann cells

The cytoplasmic ATP concentration is in the range 5–10 mM and there is little doubt that the $P2X_7$ receptor, first described as a cytolytic ATP receptor (Surprenant *et al*., 1996), can be activated when ATP is massively released by any dying cell. However, until recently, the main obstacle for the attribution of more physiological roles for $P2X_7$ receptors was the lack of data showing that these receptors could be activated by nonlytic release of ATP. Using multicompartment cell cultures chambers allowing chronic electrical stimulation, Stevens & Fields (2000) have estimated the concentration of ATP released along stimulated DRG axons to ≈ 14.5 nM which they assumed to correspond to a 10^{-7}–10^{-8}-fold dilution of the ATP produced within the axon–Schwann cell intercellular space. Therefore, at least under these conditions, ATP released by nonlytic pathways may rise in the periaxonal space to a sufficient level to activate $P2X_7$ receptors expressed by ensheathing Schwann cells.

A most promising route of investigation might be the study of the involvement of the $P2X_7$ receptor in the immune functions of Schwann cells. Indeed, the $P2X_7$ is involved in several processes relevant to inflammation and immunomodulation in immune cells (DiVirgilio *et al*., 1998). During inflammation, ATP can be released by nonlytic pathways from cells primed with lipopolysaccharide (LPS) and in turn activates $P2X_7$ receptors by autocrine and paracrine loops (Ferrari *et al*., 1997b). This stimulation caused cultured mouse microglia to release the proinflammatory cytokine IL-1β through the activation of the interleukin-1-converting enzyme (ICE) (Ferrari *et al*., 1996; Sanz & DiVirgilio, 2000). Although not completely clear, the pathways leading to the activation of ICE involved a decrease in cytoplasmic K^+ (Perregaux & Gabel, 1994; Cheneval *et al*., 1998).

In the PNS, LPS-primed Schwann cells are also capable of synthesizing and releasing interleukin-1 β (IL-1β) (Bergsteinsdottir *et al*., 1991; Skundric *et al*., 1997) but the putative role of the $P2X_7$ receptor in such mechanisms remains to be investigated. An attractive hypothesis would be that, during pathological events, ATP acting on Schwann cell $P2X_7$ receptors induces the maturation and the release of IL-1β. The Ca^{2+}-dependent K^+ conductance could represent a novel pathway for a $P2X_7$-mediated K^+ efflux and may modulate the ability of Schwann cells to synthesize and release proinflammatory cytokines. In conclusion, the different conductances activated by $P2X_7$ receptors on mouse Schwann cells may participate to an integrated regulation of inflammatory processes during nerve injury or peripheral neuropathies.

Acknowledgements

We thank Dr Florence Pousset, Dr Nathalie Chauvet, Dr Patricia Parnet and Danielle Verrier for microglial cell cultures and help in immunocytochemistry. We are very grateful to Dr Stéphane Oliet and Dr Frédéric Nagy for reading and helpful comments on this manuscript. Supported in part by the Ligue Française contre la Sclérose en Plaques.

Abbreviations

ATP, adenosine 5′-triphosphate; BAPTA, 1,2-bis (2-aminophenoxy) ethane-N,N,N',N′-tetraacetic acid; BK channels, large conductance Ca^{2+}-activated K^+ channels; BzATP, 2′,3′-O-(4-benzoyl-4-benzoyl)-ATP; ChTX, charybdotoxin; E_{ATP}, reversal potential of the ATP-activated current; EGTA, 10 ethylene-glycol-bis (β-aminoethylether)-N,N′-tetraacetic acid; ICE, interleukin-1-converting enzyme; IFNγ, interferon gamma; IL-1β, interleukin 1 beta; LPS, lipopolysaccharide; oATP, periodate oxidized ATP; PBS, phosphate-buffered saline; SCN^-, thiocyanate; TEA, tetraethylammonium; TNFα, tumour necrosis factor alpha.

References

Amédée, T., Colomar, A. & Coles, J.A. (2001) ATP signalling in Schwann cells. In De Vellis, J. (ed.), *Neuroglia in the Aging Brain*. Humana Press, Totowa, NJ, USA (in press).

Amédée, T. & Despeyroux, S. (1995) ATP activates cationic and anionic conductances in Schwann cells cultured from dorsal root ganglia of the mouse. *Proc. Roy. Soc. Lond. B*, **259**, 277–284.

Amédée, T., Ellie, E., Dupouy, B. & Vincent, J.D. (1991) Voltage-dependent calcium and potassium channels in Schwann cells cultured from dorsal root ganglia of the mouse. *J. Physiol. (Lond.)*, **441**, 35–56.

Beaudu-Lange, C., Despeyroux, S., Marcaggi, P., Coles, J.A. & Amédée, T. (1998) Functionnal Ca^{2+} and Na^+ channels on mouse Schwann cells cultured in serum-free medium: regulation by a diffusible factor from neurons and by cAMP. *Eur. J. Neurosci.*, **10**, 1796–1809.

Bergsteinsdottir, K., Kingston, A., Mirsky, R. & Jessen, K.R. (1991) Rat Schwann cells produce interleukin-1. *J. Neuroimmunol.*, **34**, 15–23.

Bevan, S., Gray, P.T.A. & Ritchie, J.M. (1984) A calcium-activated cation-selective channel in rat cultured Schwann cells. *Proc. Roy. Soc. Lond. B*, **222**, 349–355.

Cheneval, D., Ramage, P., Kastelic, T., Szelestenyi, T., Niggli, H., Hemmig, M., Bachmann, M. & MacKenzie, A. (1998) Increased mature interleukin-1β secretion from THP-1 cells induced by nigericin is a result of activation of p45 IL-1β-converting enzyme processing. *J. Biol. Chem.*, **273**, 17846–17851.

Cohn, M. (1990) Structural and chemical properties of ATP and its metal complexes in solution. *Ann. N.Y. Acad. Sci.*, **603**, 151–164.

Coutinho-Silva, R., Persechini, P.M., Da Cunha Bisaggio, R., Perfettini, J.L., Torres De, Sa, Neto, A.C., Kanellopoulos, J.M., Motta-Ly, I., Dautry-Varsat, A. & Ojcius, D.M. (1999) P2Z/$P2X_7$ receptor-dependent apoptosis of dendritic cells. *Am. J. Physiol.*, **276**, C1139–C1147.

DiVirgilio, F., Chiozzi, P., Falzoni, S., Ferrari, D., Sanz, J.M., Venketaraman, V. & Baricordi, O.R. (1998) Cytolytic P2X purinoceptors. *Cell Death Differentiation*, **5**, 191–199.

Ferrari, D., Chiozzi, P., Falzoni, S., Hanau, S. & DiVirgilio, F. (1997b) Purinergic modulation of interleukin-1β release from microglial cells stimulated with bacterial endotoxin. *J. Exp. Med.*, **185**, 579–582.

Ferrari, D., Chiozzi, P., Falzoni, S., Susino, M.D., Collo, G., Buell, G. & DiVirgilio, F. (1997a) ATP-mediated cytotoxicity in microglial cells. *Neuropharmacology*, **36**, 1295–1301.

Ferrari, D., Villalba, M., Chiozzi, P., Falzoni, S., Ricciardi-Castagnoli, P. & DiVirgilio, F. (1996) Mouse microglial cells express a plasma membrane pore gated by extracellular ATP. *J. Immunol.*, **156**, 1531–1539.

Grafe, P., Mayer, C., Takigawa, T., Kamleiter, M. & Sanchez-Brandelik, R. (1999) Confocal calcium imaging reveals an ionotropic P2 nucleotide receptor in the paranodal membrane of rat Schwann cells. *J. Physiol. (Lond.)*, **515**, 377–383.

Gray, P.T., Bevan, S. & Ritchie, J.M. (1984) High conductance anion-selective channels in rat cultured Schwann cells. *Proc. Roy. Soc. Lond. B*, **221**, 395–409.

Haas, S., Brockhaus, J., Verkhratsky, A. & Kettenmann, H. (1996) ATP-induced membrane currents in ameboid microglia acutely isolated from mouse brain slices. *Neuroscience*, **75**, 257–261.

Humphreys, B.D. & Dubyak, G.R. (1996) Induction of the P2z/P2X7 nucleotide receptor and associated phospholipase D activity by lipopolysaccharide and IFN-gamma in the human THP-1 monocytic cell line. *J. Immunol.*, **157**, 5627–5637.

Humphreys, B.D. & Dubyak, G.R. (1998) Modulation of P2X7 nucleotide receptor expression by pro- and anti-inflammatory stimuli in THP-1 monocytes. *J. Leukoc. Biol.*, **64**, 265–273.

King, B.F., Townsend-Nicholson, A., Wildman, S.S., Thomas, T., Spyer, K.M. & Burnstock, G. (2000) Coexpression of rat $P2X_2$ and $P2X_6$ subunits in Xenopus oocytes. *J. Neurosci.*, **20**, 4871–4877.

Lê, K.T., Babinski, K. & Séguéla, P. (1998) Central P2X4 and P2X6 channel subunits coassemble into a novel heteromeric ATP receptor. *J. Neurosci.*, **18**, 7152–7159.

Lewis, C., Neidhart, S., Holy, C., North, R.A., Buell, G. & Surprenant, A. (1995) Coexpression of $P2_X2$ and P2X3 receptor subunits can account for ATP-gated currents in sensory neurons. *Nature*, **377**, 432–435.

McCarty, N.A. (2000) Permeation through the CFTR chloride channel. *J. Exp. Biol.*, **203**, 1947–1962.

Mi, H., Harris-Warrick, R.M., Deerinck, T.J., Inman, I., Ellisman, M.H. & Schwarz, T.L. (1999) Identification and localization of Ca^{2+}-activated K+ channels in rat sciatic nerve. *Glia*, **26**, 166–175.

Mutini, C., Falzoni, S., Ferrari, D., Chiozzi, P., Morelli, A., Baricordi, O.R., Collo, G., Ricciardi-Castagnoli, P. & Di Virgilio, F. (1999) Mouse dendritic cells express the $P2X_7$ purinergic receptor: characterization and possible participation in antigen presentation. *J. Immunol.*, **163**, 1958–1965.

Pérez-Samartin, A.L., Miledi, R. & & Arenallo, R.O. (2000) Activation of volume -regulated Cl^- channels by Ach and ATP in *Xenopus* follicles. *J. Physiol. (Lond.)*, **525**, 721–734.

Perregaux, D. & Gabel, C.A. (1994) Interleukin-1β maturation and release in response to ATP and nigericin. *J. Biol. Chem.*, **269**, 15195–15203.

Pousset, F., Palin, K., Verrier, D., Poole, S., Dantzer, R., Parnet, P. & Lestage, J. (2000) Production of IL-1 receptor antagonist isoforms by microglia in mixed rat glial cells stimulated by lipopolysacharide. *Eur. Cytokine. Netw.*, **11**, 682–689.

Quasthoff, S., Strupp, M. & Grafe, P. (1992) High conductance anion channel in Schwann cell vesicles from rat spinal roots. *Glia*, **5**, 17–24.

Ralevic, V. & Burnstock, G. (1998) Receptors for purines and pyrimidines. *Pharmacol. Rev.*, **50**, 413–492.

Sanz, J.M. & DiVirgilio, F. (2000) Kinetics and mechanism of ATP-dependent IL-1β release from microglial cells. *J. Immunol.*, **164**, 4893–4898.

Skundric, D., Bealmear, B. & Lisak, R.P. (1997) Inducible IL-1α, IL-1β, IL-1R and IL-1 receptor antagonist (RA) expression in cultured rat Schwann cells (SC). *J. Neurochem.*, **64**, S69.

Solini, A., Chiozzi, P., Morelli, A., Fellin, R. & DiVirgilio, F. (1999) Human primary fibroblasts in vitro express a purinergic $P2X_7$ receptor coupled to ion fluxes, microvesicle formation and IL-6 release. *J. Cell. Sci.*, **112**, 297–305.

Steinert, M. & Grissmer, S. (1997) Novel activation stimulus of chloride channels by potassium in human osteoblasts and human leukaemic T lymphocytes. *J. Physiol. (Lond.)*, **500**, 653–660.

Stevens, B. & Fields, R.D. (2000) Response of Schwann cells to action potentials in development. *Science*, **287**, 2267–2271.

Surprenant, A., Rassendren, F., Kawashima, E., North, R.A. & Buell, G. (1996) The cytolytic P_{2Z} receptor for extracellular ATP identified as a P_{2X} receptor ($P2X_7$). *Science*, **272**, 735–738.

Torres, G.E., Haines, W.R., Egan, T.M. & Voigt, M.M. (1998) Co-expression of $P2X_1$ and $P2X_5$ receptor subunits reveals a novel ATP-gated ion channel. *Mol. Pharmacol.*, **54**, 989–993.

Vinogradova, I.M., Philippi, M. & Amédée, T. (1994) ATP activates a membrane current in frog (Rana pipiens) Schwann cells. *J. Physiol. (Lond.)*, **480**, 35P.

Virginio, C., MacKenzie, A., North, R.A. & Surprenant, A. (1999) Kinetics of cell lysis, dye uptake and permeability changes in cells expressing the rat $P2X_7$ receptor. *J. Physiol. (Lond.)*, **519**, 335–346.

Wiley, J.S., Cargett, C.E., Zhang, W., Snook, M.B. & Jamieson, G.P. (1998) Partial agonists and antagonists reveal a second permeability state of human lymphocyte P2Z/$P2X_7$ channel. *Am. J. Physiol.*, **275**, C1224–C1231.

Zeng. W., Lee, M.G. & Muallem, S. (1997) Membrane-specific regulation of Cl^- channels by purinergic receptors in rat submandibular gland acinar and duct cells. *J. Biol. Chem.*, **272**, 32956–32965.